CNRS
Centre National de la Recherche Scientifique

INFN
Istituto Nazionale di Fisica Nucleare

AdV SLC: Characterization of Silicon Carbide for constructing baffles and beam dumps in AdV

VIR-0460A-12

Antonino Chiummo*, Benjamin Canuel, Andrea Magazzu, and Julien Marque

EGO - European Gravitational Observatory

Date: November 22, 2012

[*] *corresponding author:* antonino.chiummo@ego-gw.it

VIRGO* A joint CNRS-INFN Project - EGO* the site of the VIRGO project
Via E. Amaldi, I-56021 S. Stefano a Macerata - Cascina (Pisa)
Secretariat: Telephone (39) 050 752 521 * FAX (39) 050 752 550 * Email: ego@ego-gw.it

Contents

Introduction **2**

1 Refractive index and Reflectivity **2**
1.1 Polished SiC sample . . . 2
1.2 Polished CVD-SiC coated sample . . . 3

2 Absorption **3**
2.1 Direct measurements . . . 3

3 Scattering **4**
3.1 Total Integrated Scattering (TIS) of samples . . . 4
3.1.1 TIS of "Brut de frittage" and ground samples . . . 4
3.1.2 TIS of polished sample . . . 4
3.1.3 TIS of CVD-SiC polished sample . . . 5
3.2 Bidirectional Reflectance Distribution Function (BRDF) of samples . . . 5
3.2.1 BRDF of "brut de frittage" sample . . . 5
3.2.2 BRDF of ground sample (with and w/o AR coating) . . . 5

4 Damage threshold and thermal behavior **6**
4.1 Thermal conduction of SiC . . . 6
4.2 In-air damage threshold of uncoated SiC . . . 6
4.3 In-air damage threshold of AR-coated SiC . . . 7
4.4 In-air damage threshold of CVD-SiC . . . 7
4.5 In-vacuum damage thresholds . . . 8

5 Edge sharpness and microscope analysis **9**

6 Outgassing **10**

7 Electric conductivity **10**

Aknowledgements **10**

References **11**

Introduction

In this document we report about the characterization of Silicon Carbide (SiC) for application in gravitational-wave interferometric antennas as beam-dump of laser power at wavelength $\lambda = 1.064 \mu m$ (Nd:YAG laser) [1]. We tested 6H-SiC by Boostec [2] with several surface finishes:

- *basic finish:* also known as *brut de frittage*, meaning the sample as it comes out from the furnace;
- *ground:* better quality than *brut de frittage*, the sample undergoes grinding of the surface. Also known as *rectifié*;
- *polished* (usually there are still microscopic holes on the surface due to SiC porosity);
- *CVD-SiC polished:* sample coated with a layer of Chemical Vapor Deposited SiC (CVD-SiC) and then polished. The deposition of a homogeneous layer of SiC by means of the CVD technique is intended to get rid of the microscopic holes at the surface.

In the following, a collection of some important features of this material are reported, along with a short description of the measurements we performed.

1 Refractive index and Reflectivity

1.1 Polished SiC sample

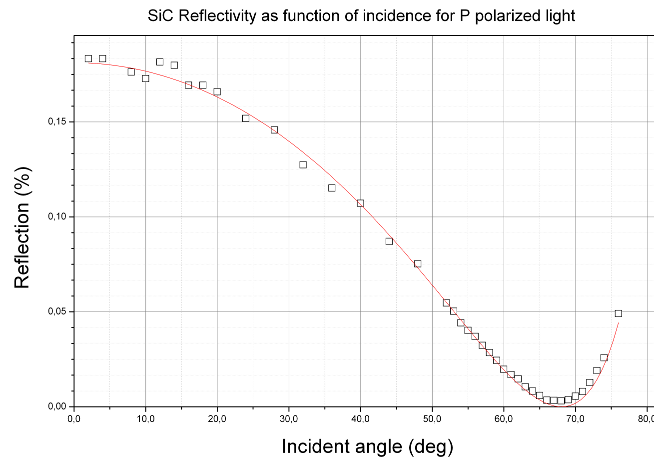

Figure 1: Polished SiC reflectivity for P-polarized light ($\lambda = 1.064 \mu m$) as a function of incident angle.

We tested the reflectivity of a polished sample of SiC as a function of incidence angle for P-polarized light in the scope of measuring its Brewster angle and estimate its refractive index. Results are given in figure 1. The Brewster angle is about 68°. Fit of the data with Fresnel law gives an optical index of 2.48. It is quite close to expected value for 6H-SiC, which is about 2.6 (goes from 2.58 to 2.62 depending on ordinary or extraordinary axis). In agreement with Fresnel law, reflectivity at normal incidence is about 18.5% (i.e. we need to coat it to use it effectively to dump light at YAG wavelenght).

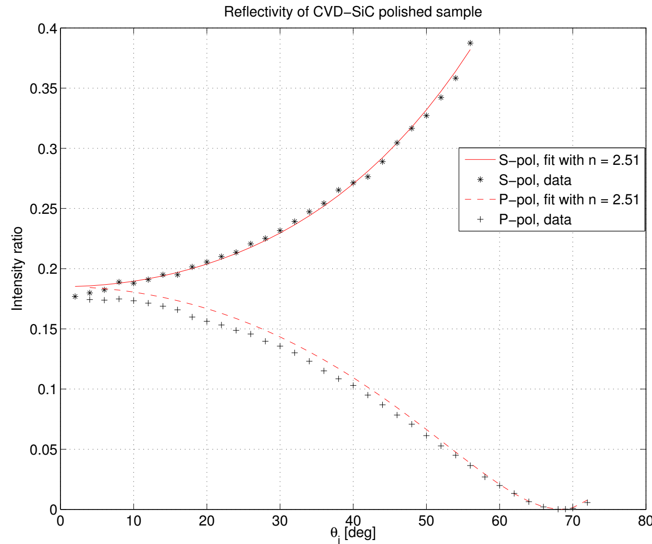

Figure 2: Polished CVD-SiC reflectivity for both P-polarized ans S-polarized light ($\lambda = 1.064\mu m$) as a function of incident angle θ_i. Stars: measured reflectivity for S-polarized light, solid red line: fit with Fresnel coefficients. Crosses: measured reflectivity for P-polarized light, dashed red line: fit with Fresnel coefficients. The refractive index was estimated by fitting the P and S polarization data at the same time: $n_{CVD-SiC} = 2.51$.

1.2 Polished CVD-SiC coated sample

We repeated the measurement as in previous paragraph, this time on the CVD-SiC polished sample and for both the P and S polarizations. Results are reported in figure 2. According to the fit with Fresnel law, the refractive index is $n_{CVD-SiC} = 2.51$, the Brewster angle is $\theta_B = 68.5°$, reflectivity at θ_B is $R_B \sim 130ppm$, and the the normal incidence reflectivity is $R_\perp = 18.5\%$. So no major differences are noticed between the two kinds of SiC realizations (chemical vapor deposited or sintered).

2 Absorption

2.1 Direct measurements

As expected for 6H-SiC, internal absorption is very high and no transmission can be measured with few-millimiter thick samples. Boostec had also given us a demonstrative sample which consist of substrate plus a layer of 300-500μm of SiC deposited by Chemical Vapor Deposition (CVD) technique. In fig.3(a) one can see the different layers this sample is made of, the outer one being the CVD-SiC. In order to measure the absorption at 1.064μm, we tried to peel the sample from the back so to have just the CVD-SiC layer (fig.3(b)). Then a laser beam was sent onto this thin layer to measure the transmitted power. Impinging power: $P_{inc} = 670mW$; assumed reflectivity: 0.18; detectability: around $50nW/550mW = 0.9ppm$. In this condition, we measured around $P_{tr} \sim 500nW$ in transmission from the sample. We tried to measure the thickness of the layer by means of a Vernier caliper, and found around 670μm. So the conclusion is that 670μm of this kind of CVD-SiC are able to stop around 550mW of a laser at 1.064μm. From this result we can derive an estimate for the absorption coefficient α of that kind of SiC (CVD-SiC):

$$P_{tr}/P_0 = \exp(-\alpha x) \Rightarrow \alpha = \frac{1}{x}\log(\frac{P_0}{P_{tr}}) \sim 2 \times 10^2 cm^{-1}$$

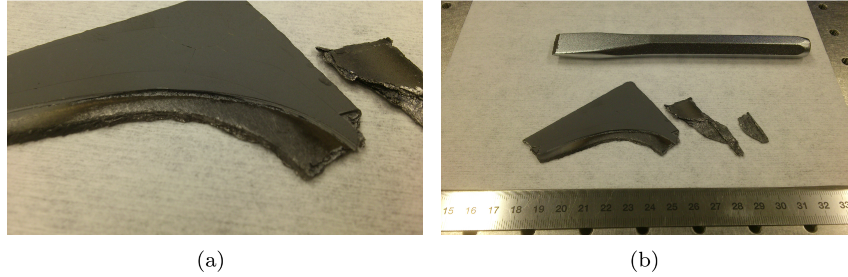

(a) (b)

Figure 3: The CVD-SiC coated sample.
(a): The outer layer is made of CVD-SiC. (b): Some fragments of the sample were peeled in order to get just the thin CVD-SiC coating.

where $P_0 = (1 - refl)\ P_{inc}$ is the impinging power that is not reflected off the sample, P_{tr} is the measured power in transmission. This value is not in agreement with other measurements usually found in literature, as absorption coefficients for sintered 6H-SiC are few cm^{-1} [3]. But the latter refer usually to sintered 6H-SiC (or other preparation methods) and not to CVD-SiC, that gives instead a very high purity of the sample. We found another measurement in literature [4] where they find an absorption coefficient around $\alpha \sim 10^2\ cm^{-1}$ at $\lambda = 1000nm$, for 6H-SiC at normal pressure, but it is unclear which kind of 6H-SiC they refer to.
With this value for the absorption coefficient, the expected imaginary part of the refractive index would be: $n_{im} = \alpha\ \lambda/4\pi \sim 1.5\ 10^{-3}$. Such a value is very small if compared with what we are able to derive from the measurement of reflectivities and Fresnel coefficients.

3 Scattering

3.1 Total Integrated Scattering (TIS) of samples

3.1.1 TIS of "Brut de frittage" and ground samples

The two samples "brut de frittage" and "rectifié" (ground) are too rough to present a clean specular reflection. We measured then the total emitted light from these samples when submitted to S-polarized light at 45° of incidence, by means of an integrating sphere. This measurement takes into account *all* the reflected light from the sample. We measured 18% and 16.7% respectively on "rectifié" and "brut de frittage".
We tested also the ground SiC diaphragms Anti-Reflective (AR) coated by CVI [5], with a single layer of SiO_2 whose thickness is optimized for $\lambda = 1.064\mu m$.

Experimental conditions: 45° incidence, S-polarized light, reference sample with 100% diffusion= 9.6mW, SiC sample diffused power= $200\mu W$, so TIS=2%, which means that the AR coating effectively decreases the scattering by a factor 8. We obtained roughly the same results also for the 0° incidence case.

3.1.2 TIS of polished sample

With the polished sample, we could separate specularly reflected from scattered light. For S-polarized light at 45° of incidence, we measured $TIS_{polished} = 6550ppm$ of diffusion. Target value to realize high power beam dump would rather be ideally less than 100ppm.

3.1.3 TIS of CVD-SiC polished sample

We tested two samples of SiC coated with CVD-SiC and polished, provided by Boostec. Measurements at 45°with an integrating sphere yielded $TIS_6^{(45^\circ)} = 20-33ppm$ for sample labelled #6, and $TIS_1^{(45^\circ)} = 20-52ppm$ for sample labelled #1. We repeated the measurement at 0°incidence and found $TIS_6^{(0^\circ)} = 10-30ppm$ for sample labelled #6, and $TIS_1^{(0^\circ)} = 33-75ppm$ for sample labelled #1, *i.e.* more or less the same results as for 45° incidence. So the total integrated scattering for those samples is TIS < 100ppm.

3.2 Bidirectional Reflectance Distribution Function (BRDF) of samples

3.2.1 BRDF of "brut de frittage" sample

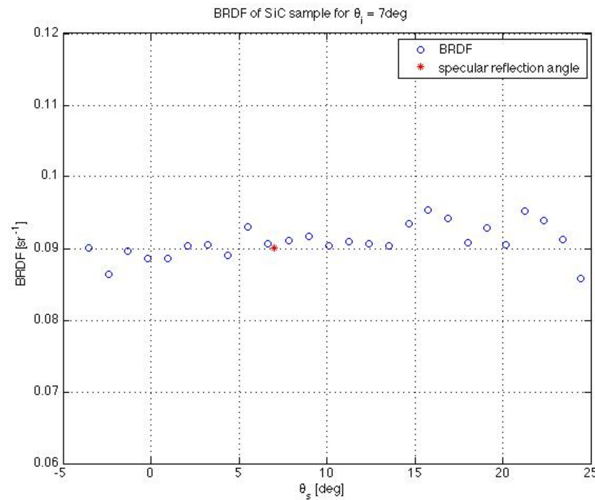

Figure 4: BRDF for the sample "brut de frittage" as a function of the scattering angle θ_s. The laser hit the sample at around 7° angle of incidence.

Later on, we measured the Bidirectional Reflectance Distribution Function (BRDF) for the sample termed "brut de frittage" when shone by a laser beam ($1.064\mu m$) at around 7° angle of incidence (θ_i). The BRDF turned out to be of the order of 0.09/sr, with a rather flat distribution for different scattering angles (θ_s), see fig.4. If the sample had been a perfect Lambertian scatterer, the BRDF should have been: $BRDF = TIS/\pi = 0.167/\pi = 0.053/sr$.

3.2.2 BRDF of ground sample (with and w/o AR coating)

We measured also the BRDF's of a SiC sample whose faces had been ground (fig.5(a)) and one face had been AR-coated too by CVI (fig.5(b)).

The results for those measurements are shown in fig.6. The BRDF of the ground face (fig.6(a)) is around 0.12/sr. This value is a bit larger than the one for the "brut de frittage". This is partly explained by the fact that the TIS of this sample is larger than the TIS of the "brut de frittage" one. Additionally, one should take into account that the roughness of the ground face is no longer totally random but shows the signs of the machining. This quasi-regular structure could in principle concentrate part of the scattered light toward a plane close to the horizontal one, where the measurement was performed. Anyway, the AR-coating on the other face effectively decreases the BRDF by a factor 8 (fig.6(b)), giving $BRDF < 0.015\ sr^{-1}$.

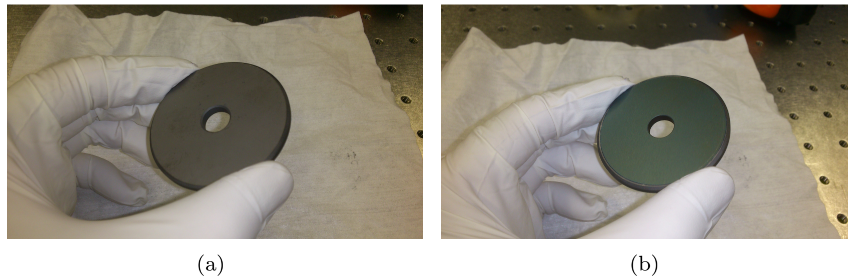

(a) (b)

Figure 5: A SiC sample to serve as a diaphragm, both faces have been ground. (a): the back face has no coating. (b): The pictured face is both ground and AR coated for 1.064um wavelength.

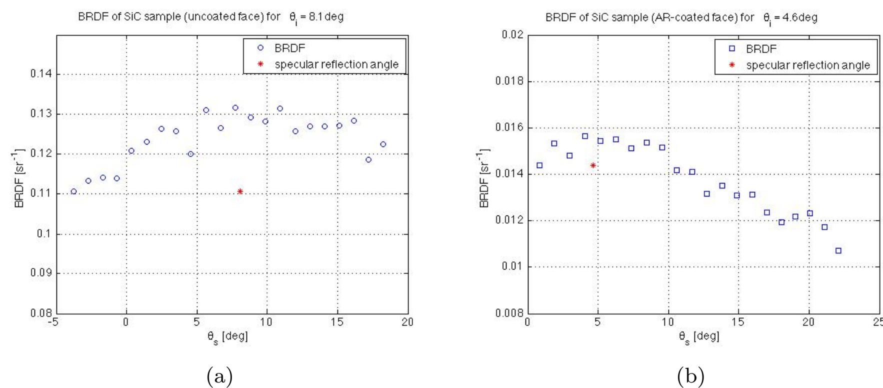

(a) (b)

Figure 6: BRDF's for the sample of fig.5 as a function of the scattering angle θ_s. (a): The back (uncoated) face's BRDF with an angle of incidence $\theta_i \sim 8°$. (b): For the AR-coated face the angle of incidence was $\theta_i \sim 5°$. The coating decreases the BRDF by a factor 8.

4 Damage threshold and thermal behavior

4.1 Thermal conduction of SiC

We measured the thermal maps of SiC and Si for an absorbed Yag laser power of about 10W. The beam waist used is about 2.5mm and is far larger than the lateral dimension of both samples (Si sample is a square of $60mm \times 60mm \times 5mm$ and SiC sample has a round shape of diameter $66mm \times 4mm$ thickness). We observe on fig.7 that thermal gradient inside SiC is much smaller than in Si. Indeed, peak to peak temperature elevation is 9°C for SiC and 24°C for Si. Therefore we expect a very good conduction coefficient for SiC (Si conduction is 150 W/m/K [6]). Indeed we find conduction values of $\sim 400W/m/K$ for 6H-SiC in literature (see for instance [7]).

4.2 In-air damage threshold of uncoated SiC

We measured the in-air damage threshold for a polished SiC sample, and made a comparison between SiC and Si. The damage threshold was measured by slowly ramping up incident power on both materials. A beam waist of $200\mu m$ and $500\mu m$ were respectively used for SiC and Si. We could measure damage threshold of $30kW/cm^2$ and $6kW/cm^2$ for SiC and Si. Figure 8 gives a view of the damage created on SiC surface for the maximum tested power (40W).

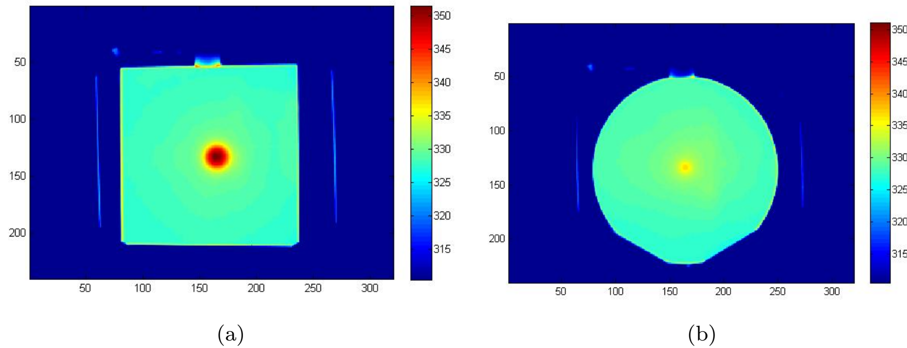

(a) (b)

Figure 7: Thermal map of Si (left) and SiC (right) for 10W of absorbed laser power. Temperature scale is in K.

Figure 8: View of the damage created on SiC surface by Yag laser beam.

4.3 In-air damage threshold of AR-coated SiC

The AR-coated ground SiC sample was exposed to the high-power YAG laser with an incident beam size of $200\mu m$. The sample was mounted in a standard 2" mount. Damage barely visible on surface starting at around 35W of incident power. Well visible mark on the surface with incident power around 40W (see fig.9(a): photo of the sample, and fig.9(b): microscope image of the spot). No damage visible with incident power up to 30W. In first approximation the reflectivity of the AR-coated sample can be neglected (few percents), and this lets us estimate a damage threshold of $\sim 28KW/cm^2$, so it seems that the coating itself does not change this parameter with respect to the uncoated sample.

4.4 In-air damage threshold of CVD-SiC

The same setup was used to investigate the polished CVD-SiC sample. This sample was too big for a standard 2" mount, so we used an adjustable filter holder. No visible signs on the surface with up to 40W of incident power (but reflectivty 18.5%, so absorbed power was around 32W). First damage noticed at 44W incident power (36W absorbed power). Figure 10(a) shows a photo of the spot marked by the laser onto the sample surface. It is interesting to notice that some kind of "coma" (tail going downward and leftward in the picture) was printed

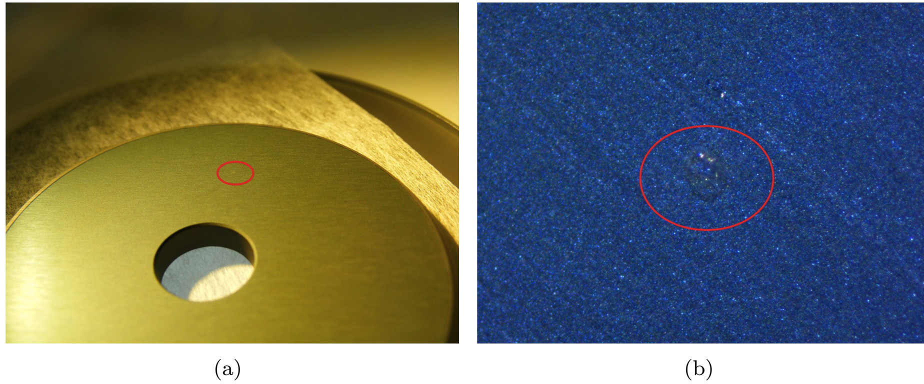

(a) (b)

Figure 9: The AR-coated ground SiC sample, after being damaged by the YAG laser. (a): the area encircled in red is where the damage occurred. (b): zoom in of previous area by means of an optical microscope. This damage occurred at an impinging power of $\sim 40W$.

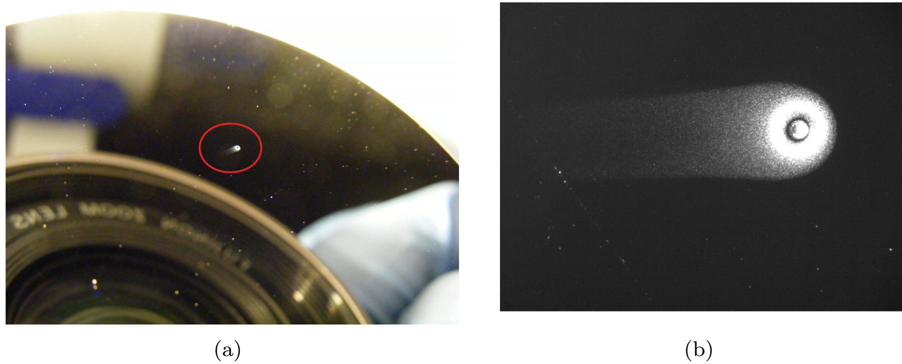

(a) (b)

Figure 10: The polished CVD-SiC coated SiC sample, after being damaged by the YAG laser. (a): the area encircled in red is where the damage occurred. (b): zoom in of previous area by means of an optical microscope. The origin of the coma-like tail is not yet fully understood.

by the laser beam onto the surface. Figure 10(b) is the same area as seen by the microscope, confirming the presence of the coma. We turned the sample by 90°, and exposed it once again to the laser beam at 44W so to check whether the direction of the tail follows the sample or not. We found that the new spot featured a coma as well, impressed more or less along the same direction in the space as last one (not in the same direction as referred to the sample). So probably this coma is a feature related to the optical setup rather than the properties of the material.
Also polished CVD-SiC coated SiC showed a damage threshold of $\sim 28KW/cm^2$, comparable with the previous samples.

4.5 In-vacuum damage thresholds

No measurements to report to date, but we do not expect a big change for the damage threshold in vacuum. In fact, as this is mostly a localized interaction, the thermal conduction from the hot spot to the rest of the sample is largely dominant with respect to the heat dissipation of the sample as a whole.

5 Edge sharpness and microscope analysis

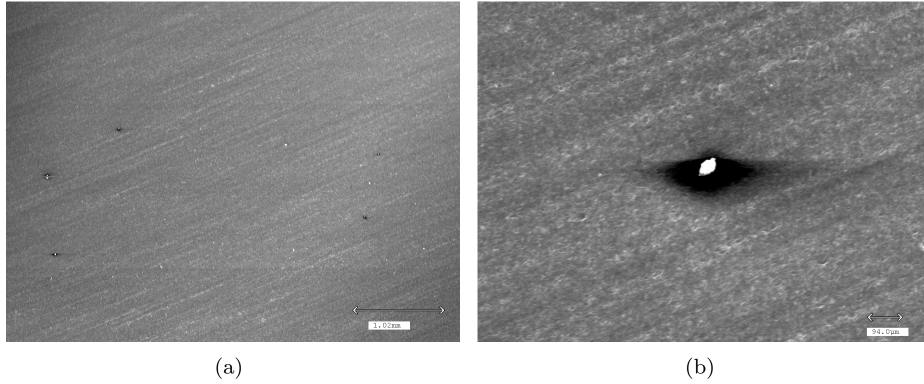

(a) (b)

Figure 11: (a): The SiC sample AR coated surface, where there are some holes due to the porosity of SiC. (b): Zoom in on one of the biggest defect.

We had the opportunity to use the Scanning Electron Microscope (SEM) in the Physics Department in Pisa. We looked at a Boostec SiC diaphragm (2 inches diameter, 5mm hole), ground surface and AR coated by CVI. Figure 11(a): looking at the AR coated surface, one can see very well some holes. Indeed, we know that SiC is porous. Figure 11(b): zoom on one of the largest hole. From this pictures we can draw a rough estimate of the total area of the holes as a ratio of the total area of the sample. Average area of the defects in picture: $A_{def} = 0.079mm^2$, number of defects in the picture: $n_{def} = 6$, area of the picture: $A_{pic} = 19.1mm^2$, ratio of total defect area over total picture area (R_{def}):

$$R_{def} = n_{def} \frac{A_{def}}{A_{pic}} = 2500ppm$$

Let us assume that all the scattering of the light occurs because of these defects and not because of the roughness

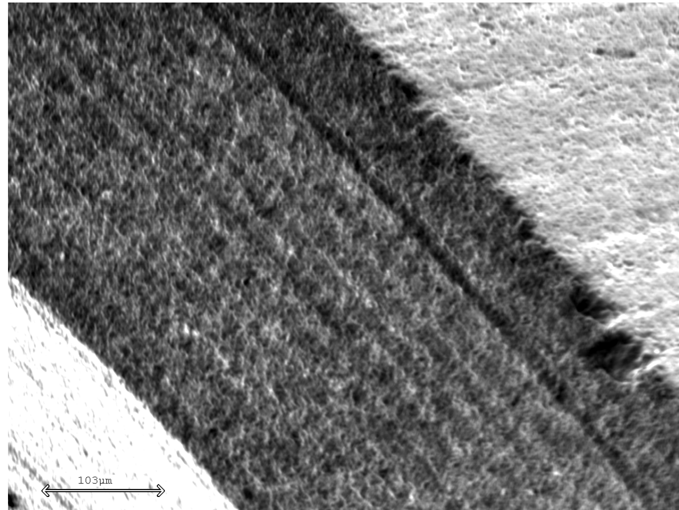

Figure 12: Detail of the AR coated surface of the SiC diaphragm. The AR coated surface is visible on the right, the 45 degrees chamfer in the middle, the internal edge of the diaphragm on the left. The sample is tilted by 45 degrees with respect to the horizontal plane.

of the sample. Let us suppose, additionally, that the polishing does not change the number and size of defects,

but just reduces the μ-roughness rms. Then we should have this figure, R_{def}, to be comparable with the TIS of the sample with the lowest roughness, *i.e.* the polished sample. Indeed we have:

$$\frac{R_{def}}{TIS_{polished}} = \frac{2500}{6550} \sim 40\%$$

As the ratio of defect area over total area is roughly half of the TIS of the polished sample, and considering the large error bar in such a kind of estimation, we cannot exclude that the TIS of the sample under investigation is mainly due to the presence of the hole defects.
Figure 12: here we see the AR coated surface on the right, the 45 degrees chamfer in the middle, the internal edge of the diaphragm on the left the sample is tilted by 45 degrees with respect to the horizontal plane. The chamfer is about $70\mu m$. Many hole defects of diameter about $50\mu m$. By looking at the image of fig.12, we could estimate the radius of curvature of the edge to be $\sim 3 - 7\mu m$.

6 Outgassing

Most of the baffles, beam dumps and diaphragms are intended to be put in ultra-high vacuum, so an important parameter to be measured is the outgassing rate of the material they are made of.
No measurements to report to date for SiC. We plan to measure the outgassing rate of Boostec SiC with a set of samples to serve expressly for this purpose. Some vacuum-compatibility tests were performed at LIGO [8] for unpolished and uncoated sintered SiC. The tests were successful, although we do not have, to date, their numerical outcomes. In a technical data sheet by Saint-Gobain Ceramics [9], they measure a residual outgassing rate of $\sim 10^{-10} Torr\ Liters/Sec/cm^2$, after 300hrs, and after heating the test coupons to 150°C in a vacuum for 100hrs. These results are referred to Sintered-Alpha (SA) grade SiC. As a comparison, outgassing rates for AR-coated absorbing glass and stainless steel are respectively $\sim 10^{-10} Torr\ Liters/Sec/cm^2$ and $\sim 10^{-12} Torr\ Liters/Sec/cm^2$ [10].

7 Electric conductivity

Silicon carbide is a semiconductor, which can be doped n-type by nitrogen or phosphorus and p-type by aluminium, boron, gallium or beryllium [11]. In a technical data sheet by Saint-Gobain Ceramics [12], referring to SA grade SiC, they measure a resistivity $\rho = 10^2 - 10^6 \Omega cm$, dependent upon dopants in Hexoloy© SA SiC that could decrease electrical resistivity. As a comparison, typical values for stainless steel 304 are: $\rho_{ss} \sim 7 \times 10^{-5}\ \Omega cm$ [13], while on the other side, resistivity for Tecapeek CF30 ranges from $\rho_p \sim 10^3\ \Omega cm$ to $\sim 10^{10}\ \Omega cm$ [14].

Aknowledgements

We wish to thank dr. Giorgio Carelli, INFN-Pisa, who kindly helped us in using the Scanning Electron Microscope in the Department of Physics of Pisa University.
We wish to thank M. Stephane Chaillot and Boostec S.A. for their very effective cooperation.

References

[1] The Virgo Collaboration, ”Advanced Virgo Technical Design Report”, 13 April, 2012 and updates; https://tds.ego-gw.it/ql/?c=8940

[2] Boostec S.A.; http://www.mersen.com/en/products/details/f/advanced-materials-and-solutions-for-high-temperature/sintered-silicon-carbide-product.html

[3] Moriaki Wakaki (Editor), Keiei Kudo(deceased) (Editor), Takehisa Shibuya (Editor), ”Physical Properties and Data of Optical Materials”, CRC Press (April 16, 2007)
see also: http://www.ioffe.rssi.ru/SVA/NSM/Semicond/SiC/optic.html

[4] Amir Rahimpour Shayan, Huseyin Bogac Poyraz, ”Laser absorption for Si and SiC”, Western Michigan University 2008;
http://www.wmich.edu/mfe/mrc/nanomfg_group.php

[5] CVI - Melles Griot;
http://www.cvimellesgriot.com/

[6] C. J. Glassbrenner and Glen A. Slack, ”Thermal Conductivity of Silicon and Germanium from 3K to the Melting Point”, Phys. Rev. 134, A1058-A1069 (1964).

[7] E. A. Burgemeister, W. von Muench, and E. Pettenpaul, ”Thermal conductivity and electrical properties of 6H silicon carbide”; J. Appl. Phys. 50, 5790 (1979);

[8] R. Martin, L. Williams, J. Gleason, P. Sainathan, M. Arain, D. Feldbaum, G. Ciani, M. Heintze, G. Mueller, D. Reitze, D. Tanner, ”IO Stray Light Analysis and Baffle Design”, February 15, 2011; LIGO-T0900486-v5.

[9] Saint-Gobain Ceramics, Technical Data Sheet Form No. B-100610;
http://www.hexoloy.com/data-sheets/thermal-components/pdf/pdf/B-1006-10.pdf

[10] A.Pasqualetti, private communication.

[11] http://en.wikipedia.org/wiki/Silicon_carbide#Electrical_conductivity, Oct. 2012

[12] Saint-Gobain Ceramics, General Literature Form No. A-12,047;
http://www.hexoloy.com/data-sheets/silicon-carbide-products/pdf/a-12047.pdf

[13] G. Cagnoli, L. Gammaitoni, J. Kovalik, F. Marchesoni, and M. Punturo, ”Eddy current damping of high Q pendulums in gravitational wave detection experiments”, Rev. Sci. Instrum., Vol. 69, No. 7, July 1998

[14] Technical Data Sheets, Ensinger;
http://www.ensinger-online.com/modules/public/datapdf/index.php?L=0&s1=TECAPEEK&s2=0&s3=SN2&s4=CF&s5=0